A Novel Energy Filter Using Semiconductor Superlattices and its Application to Tunneling Time Calculations

Hsin-Han Tung and Chien-Ping Lee, *Senior Member, IEEE*

***Abstract*—An artificial quantum-mechanical filter using superlattice structures is proposed in this paper. By gradually changing the barrier widths of a superlattice according to a Gaussian function, a broad-band and almost zero sidelobe transmission profile can be obtained. The WKB approximation is applied to demonstrate the phenomena of abrupt change of transmission profile. The proposed structure allows the incident electrons to be nearly totally transmitted when the impinging electron energy is in the passband. On the other hand, a complete reflection occurs when the impinging energy is in the stopband. By adjusting the structure parameters, the desired passband and stopband of such a filter can be obtained. Time evolution of an electron wavepacket moving through the structure is calculated by numerically solving the time-dependent Schrödinger equation. Numerical results clearly demonstrate the characteristics of total transmission and reflection. By simulating the movement of a totally transmitted wavepacket, ambiguity results from the nature of the wavepacket in the determination of electron tunneling time can be avoided. The generalized concept of matched quantum-mechanical wave impedance (QMWI) analogous to transmission line theory is presented to explaine the occurrence of total transmission of the proposed structure. The tunneling time (τ_{QMWI}) calculated based on the concept of QMWI is compared with the accurate tunneling time obtained by our simulation.**

I. Introduction

RECENTLY, we have proposed a novel superlattice structure for energy bandpass filter (EBPF) [1]. Such a structure with a Gaussian superlattice potential profile allows the incident electrons to be nearly totally transmitted when the impinging electron energy is in the passband. On the other hand, a complete reflection occurs when the impinging energy is in the stopband. The structure can be considered as a regular superlattice with the potential modulated by a Gaussian function. A similar technique has already been used to suppress the sidelobe for the optical grating filter [2]. With the advances in the technology of molecular beam expitaxy (MBE), it is possible to control the film growth in a monolayer scale. Investigation of the propagation of electron waves in such a layered medium is of particular interest because the transport property is governed by the minibands formed in the superlattices. Multiple quantum barriers that enhance carrier blocking [3], [4] and resonant tunneling structures that enhance carrier transmission [5] are good examples that demonstrate the current manipulating capability of these structures. In this paper, another broad-band EBPF with similar transmission characteristics is presented. The bands are flat and their positions and bandwidths are adjustable. The new structure, unlike the previously proposed EBPF, has constant barrier heights but a variable barrier width, so it can be much more easily realized by epitaxial growth techniques. Details of the superlattice structure and transmission characteristics are given in Section II.

In Section III, the WKB approximation, which takes advantage of the fact that the local minibands formed in the graded structure are changing slowly, is applied to demonstrate the abrupt change of the transmission profile. In Section IV, we present results on numerical simulations of a wavepacket moving through such a structure to demonstrate the special band-passing characteristics of EBPF. At the same time, we also investigate the electron tunneling time. The physical meaning and difficulty of trying to extract the tunneling time from wavepacket simulation are discussed. The special transmission characteristics of EBPF make it possible for precise determination of the tunneling time.

In Section V, the theory of quantum-mechanical wave impedance (QMWI) is used to compute the transmission spectrum and explain the occurrence of total transmission of the proposed structure. It also calculates the electron tunneling time using the equation derived from the concept of QMWI. Finally, a conclusion is given in Section VI.

II. Structure of EBPF and Transmission Spectrum

Fig. 1 shows the schematic conduction-band diagram of the proposed structure, where a and b are the widths of the potential barriers and the wells, respectively, and V_o is the potential barrier height. The period, $a + b$, is kept constant throughout the structure but the ratio $a/a + b$ is varied according to a modulated Gaussian function. Consider one of the examples with the structure shown in Fig. 1. The superlattice is composed of 61 layer-pairs with a barrier height $V_o = 0.25$ eV. The period $a + b$ is equal to 50 Å, and the total length of the structure L is 3050 Å. The barrier width is varied gradually according to a Gaussian function $a_i = [(a+b)/2] \exp[-(i-31)^2/\sigma_x^2]$, where a_i is the width of the ith barrier, and σ_x is chosen to be 10. The calculated transmission probability by the transfer-matrix method [6] is plotted as

Manuscript received March 25, 1996; revised July 2, 1996. This work was supported by the National Science Council of the Republic of China under Contract NSC84-2215-E009-039.

The authors are with the Department of Electronics Engineering, National Chiao Tung University, Hsin Chu, Taiwan, R.O.C.

Publisher Item Identifier S 0018-9197(96)08657-5.

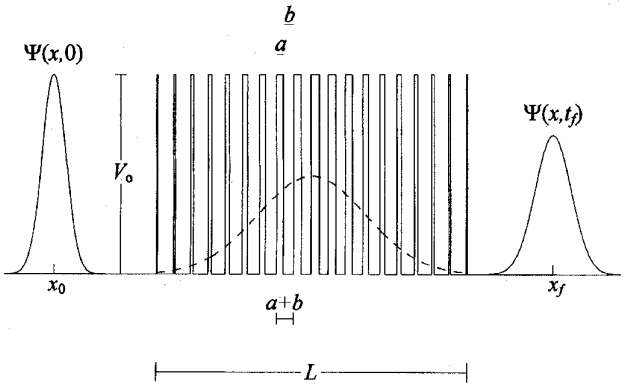

Fig. 1. Schematic conduction band-edge diagram of the proposed superlattice structure which is used for numerical calculation of electron tunneling time later. $\Psi(x,0)$ stands for the initial Gaussian wavepacket and $\Psi(x,t_f)$ is the transmitted wavepacket. The dashed line represents the function $V_M(x)$ of the first forbidden band-edge in the superlattices.

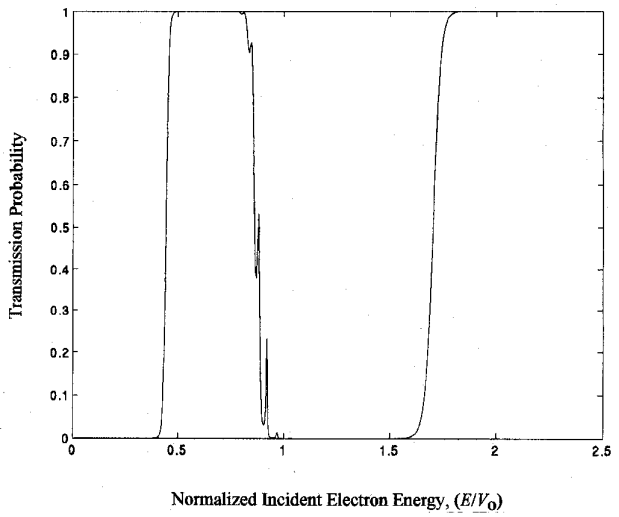

Fig. 2. Plot of the transmission probability as a function of normalized incident electron energy for the structure shown in Fig. 1, where $a+b=$ 50 Å, $V_o = 0.25$ eV, and periods $= 61$.

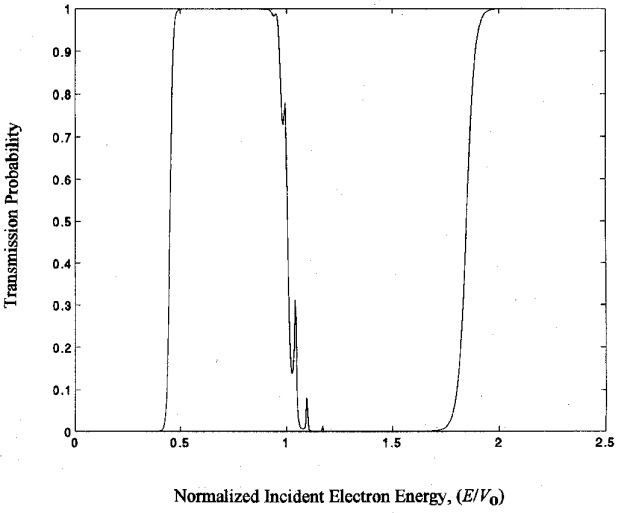

Fig. 3. Plot of the transmission probability as a function of the normalized incident electron energy for the structure shown in Fig. 1, where $a+b=60$ Å, $V_o = 0.15$ eV, and periods $= 61$.

a function of the electron energy and is shown in Fig. 2. This figure shows nearly total transmission when the electron energy is in the range between 0.5 V_o to 0.8 V_o and above 1.8 V_o, while the transmission probability is zero when the electron energy lies outside these ranges. Flat passbands and stopbands result. These characteristics are quite different from those of a conventional distributed Bragg reflector (DBR), in which the transmission bands are never totally flat. Since in our structure the barrier width is changed gradually, the minibands formed within the superlattice are expected to be changed in the same way. From the basic quantum theory [7], we know that when electrons are moving in a region where the spatial variation of potential is small compared with the electron wavelength, the reflection is expected to be small. By combining a slowly varying potential with a periodic superlattice which exhibits miniband structures, we thereby obtain a broad-band transmission profile. This superlattice structure behaves like an energy band-pass filter, which is similar to the frequency band-pass filter in an electronic circuit. This is quite different from the transmission characteristics of the conventional superlattice structures. If the structure parameters are changed to $V_o = 0.15$ eV and $a+b=60$ Å, the calculated transmission profile is shown in Fig. 3, both the band position and bandwidth change. One can get the desired transmission probability spectrum by adjusting the parameters such as $V_o, a+b$, etc.

III. The WKB Approximation

The novel feature of the present structure is that its layer thickness ratio r $(= a/a+b)$ gradually changes along the stacking direction. It is convenient to treat such inhomogeneous material system in terms of the graded minibands which are associated with the ratio r and the barrier height V_o. The graded minibands can be constructed by continuously joining the local minibands formed in each individual section. It was shown in [8] that the height of the graded barrier of the first forbidden band varies linearly with the layer thickness ratio r and reaches its maximum about $V_o/2$ when r is 0.5, or when the thicknesses of a and b are equal. In the present case, the calculated barrier edge $V_M(x)$ also varies according to the modulated Gaussian function and is shown in Fig. 1. For the convenience of calculation, we approximate $V_M(x)$ by a truncated parabolic function

$$V_M(x) = \begin{cases} \dfrac{V_o}{2}\left[1-\left(\dfrac{2}{L}x\right)^2\right], & -L/2 \le x \le L/2 \\ 0, & \text{otherwise.} \end{cases}$$

The WKB approximation is then used to calculate the transmission probability for electron incident energies E less than $V_o/2$. The transmission probability T is calculated by the

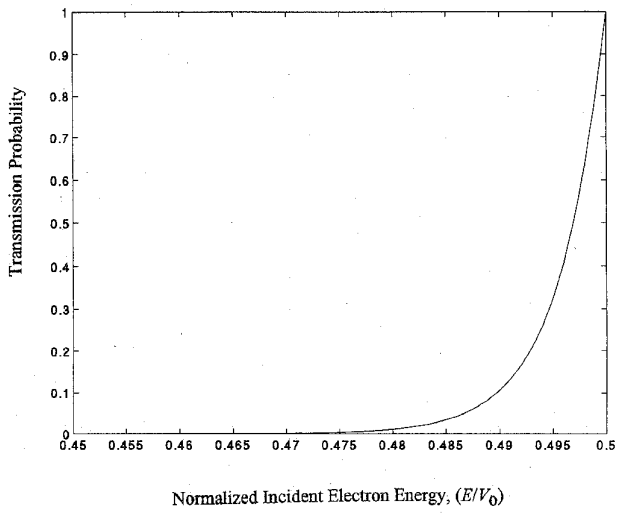

Fig. 4. Plot of the transmission probability $T(E)$ with the application of the WKB approximation for the structure shown in Fig. 1. The structure parameter is the same as that used in Fig. 2.

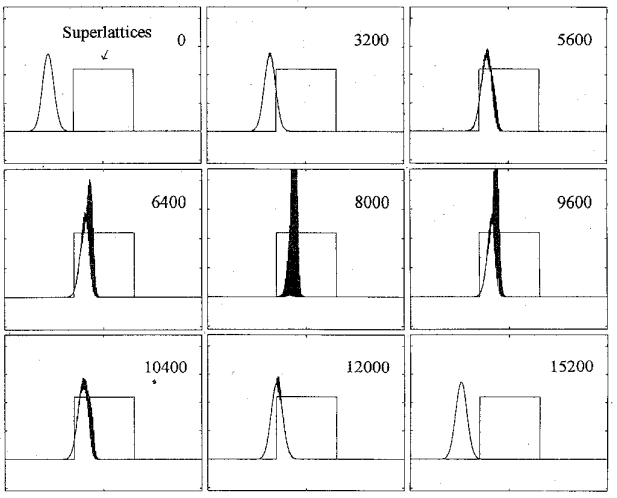

Fig. 5. Time evolution of a Gaussian wavepacket scattering from the proposed structure with the layer parameters used in Fig. 2. The average incident energy is 1.25 V_o. Numbers in each configuration denote the time in the unit of 2.316×10^{-17} s. The region enclosed by rectangle is the superlattices as shown in Fig. 1.

formula [9]

$$T = \frac{4}{\left(2\theta + \frac{1}{2\theta}\right)^2} \approx \frac{1}{\theta^2}, \qquad \theta \gg 1$$

where

$$\theta = \exp\left(\int_{-(L/2)}^{L/2} \sqrt{\frac{2m(V_M(x) - E)}{\hbar^2}}\, dx\right).$$

Substituting $V_M(x)$ into the above equation and evaluating the integral, we get

$$T(E) = \exp\left(-\frac{2\pi L}{\hbar}\sqrt{\frac{m}{V_o}}\left(\frac{V_o}{2} - E\right)\right), \qquad \theta \gg 1.$$

Using the structure parameters in Fig. 2, the calculated $T(E)$ is shown in Fig. 4. As we can see, the transmission probability increases rapidly with E and is very sensitive to E when the incident energy is near $V_o/2$. Ninety percent of the change in the transmission coefficient takes place when the incident energy is between 0.49 to 0.5 of V_o. The derived analytic expression for $T(E)$ gives a reasonable explanation why the EBPF has an abrupt transition region between the stopband and passband.

IV. Time Evolution of Wavepacket Through EBPF and Tunneling Time Calculations

A. Wavepacket Simulations

Time evolution of an electron wavepacket propagating through the proposed structure is calculated by numerically solving the Schrödinger equation. Our work follows closely that of Goldberg *et al.* [10]. The one-dimensional time-dependent wave equation is transformed into a set of difference equations, which are solved with the initial condition $\Psi(x,0) = \exp(ik_0x)\exp[-(x - x_0)^2/2\sigma_0^2]$ (see Fig. 1). We see that this packet is centered at $x = x_0$ with a spread in x governed by σ_0. The factor $\exp(ik_0x)$ indicates our initial wavepacket move to the positive direction with an average momentum $\hbar k_0$, and k_0 is equal to $\sqrt{2mE}/\hbar$, where E is the average energy of the electron wavepacket. The electron effective mass is assumed to be $0.067m_0$ throughout the structure. Fig. 5 shows the time evolution of a Gaussian wavepacket impinging upon a structure, which is the same as that used for Fig. 2. The average incident energy of the wavepacket is chosen to be 1.25 V_o and the spread σ_0 of the packet is 400 Å, which corresponds to an energy uncertainty of about 0.03 eV. From Fig. 2, we know that the incident energy of the wavepacket lies within the stopband of the transmission spectrum. Fig. 5 shows clearly that the wavepacket is totally reflected although the average incident energy is greater than the potential barrier height. If the initial wavepacket moves to the right with an incident energy $E = 0.65\ V_o$ and a same width of 400 Å (this corresponds to an energy uncertainty about 0.02 eV), i.e., when the incident energy lies in the passband of the transmission spectrum, the time evolution of the wavepacket, shown in Fig. 6 (the solid line), is totally different. Complete transmission happens and no noticeable reflection is detected. From the numerical results presented here, it is clear that the proposed structure can really serve as energy bandpass filters for electrons.

B. Tunneling Time Calculations

The question of "how long does it take for an electron to tunnel through the classically forbidden region?" has been a long-standing controversy in quantum mechanics. It is fundamental and important to quantify the electron traversal time since it limits the maximum operating speed of many modern electronic devices. Several approaches have been proposed

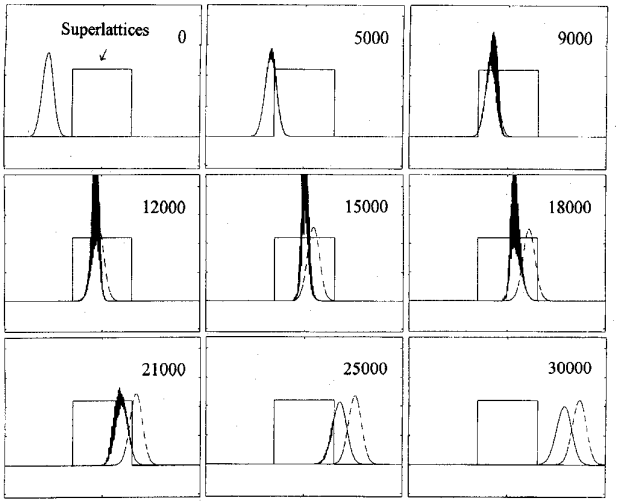

Fig. 6. Time evolution of a Gaussian wavepacket scattering from the proposed structure with the layer parameters used in Fig. 2. The average incident energy is 0.65 V_o. The free wavepacket is presented by the dotted line.

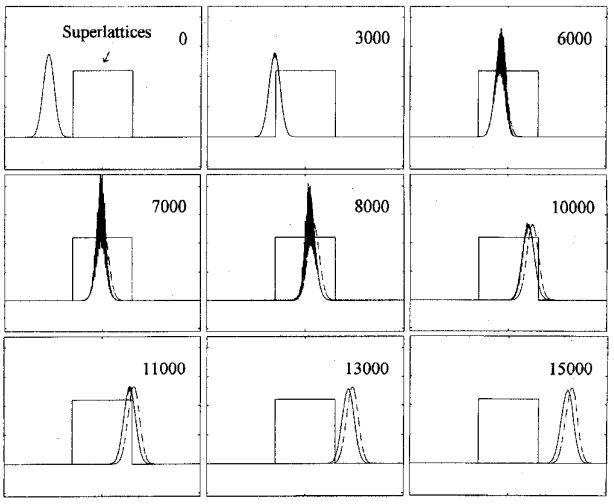

Fig. 7. Time evolution of a Gaussian wavepacket scattering from the proposed structure with the layer parameters used in Fig. 2. The average incident energy is $2.25V_o$. The free wavepacket is presented by the dotted line.

[11]–[17]. Different approaches lead to different results and the debates still exist.

The attempts to extract electron tunneling time by following the transmitted wavepacket is, however, not so successful. Generally, there are two ways to determine the tunneling time of an electron from wavepacket simulation.

1) Follow the peak of the transmitted wavepacket (i.e., the maximum of the square of the wavepacket) to determine the location x of the packet at time t. Actually, this is the same as the original idea of phase time calculation [11], but the transmitted packet may be considerably deformed and defining its peak may become ambiguous.
2) Evaluating the expectation value of the position from the transmitted packet (i.e., the center of mass) [18], [19]. This seems to give a more reliable result, but the transmission spectrum usually shows an asymmetrical profile and the mean energy of the transmitted packet may be shifted toward higher energies (the reflected packet is shifted to lower energies because of energy conservation), which makes the derivation of tunneling time somewhat ambiguous.

So, using either method, it is difficult to obtain the mean transmission time from the wavepacket simulation.

The difficulties mentioned above can be overcome if we use the EBPF to study the electron tunneling time. The special transmission characteristics of this structure make it possible for precise determination of the tunneling time. Since the wavepacket with a finite space spread Δx and a wave vector spread Δk can be 100% transmitted even when the incident energy is smaller than the barrier height, there would be no uncertainty in the evaluation of electron tunneling time. We again use the EBPF with the transmission characteristics shown in Fig. 2 in our calculation. The intrinsic tunneling time is obtained by substrating the time of free motion outside the energy filter from the total propagation time. As shown in Fig. 1, it is calculated as

$$\tau_{\rm wp} = t_f - \frac{(x_f - x_0) - L}{v}$$

where x_f is the final position of the transmitted wavepacket, t_f is the total simulation time, and $v = \sqrt{2E/m}$ is the free-electron velocity. We first consider the situation that the impinging electron energy $E = 0.65V_o$, which is smaller than the barrier height. The time evolution of the wavepacket is shown in Fig. 6. Notice the number in each frame denotes the time in the unit of 2.316×10^{-17} s. The calculated wavepacket tunneling time $\tau_{\rm wp}$ is 0.4072 ps. In Fig. 6, we also show the time evolution of the wavepacket in the absence of the filter (dashed line). The calculated free traveling wavepacket time $\tau_{\rm free}$ $(= L/v)$ is 0.3277 ps, which is smaller than the tunneling time in the presence of the EBPF. Although the scattering strength is strong when the wavepacket is moving within the superlattices, there is no distortion for the transmitted wave except the spreading of the wavepacket. This is of great advantage since the peak, stationary-phase point, and the center of mass of the transmitted packet all correspond to the same position. The ambiguity and the difficulty in determining the location of the transmitted packet are avoided. In the case of $E > V_o$ with $E = 2.25V_o$, the time series of the moving wavepacket is shown in Fig. 7. The calculated $\tau_{\rm wp}$ is 0.1891 ps, which is again greater than $\tau_{\rm free}$ $(= 0.1762$ ps). It is noticed from Figs. 6 and 7 that not only is the tunneling time longer, but the wavepacket emerged from the EBPF is also wider than the free traveling wavepacket. From the time delay and the broadening of the transmitted wavepacket compared with the free moving wavepacket, we can see that tunneling through an EBPF is like a free particle moving across a region with an effective length longer than the barrier region, and the extra length is due to the electron bouncing back and forth within the energy filter.

V. Quantum-Mechanical Wave Impedance (QMWI) and τ_{QMWI}

A. Quantum-Mechanical Wave Impedance Matching

The occurrence of broad-band transmission can be also explained using the generalized concept of matched quantum-mechanical wave impedance (QMWI) [20]. This concept is analogous to the impedance in the well-developed transmission line theory. The QMWI at any plane x can be defined as

$$Z(x) = \frac{2\hbar}{jm}\frac{\Psi'(x)}{\Psi(x)}$$

where $Z(x)$ is the wave impedance looking into the positive x direction, $j = \sqrt{-1}$, and $\Psi(x)$ and $\Psi'(x)$ are the electron wave function and its spatial derivative, respectively, for the problem interested. For an arbitrary-shaped potential, we can approximate the potential and effective mass by multistep functions with a sequence of N segments. Thus, if x_i and x_{i+1} are the boundaries of segment i, the QMWI at x_i can be calculated by

$$Z(x_i) = Z_{0i}\frac{Z(x_{i+1})\cosh(\gamma_i l_i) - Z_{0i}\sinh(\gamma_i l_i)}{Z_{0i}\cosh(\gamma_i l_i) - Z(x_{i+1})\sinh(\gamma_i l_i)}$$

where

$$\gamma_i = j\sqrt{(2m_i/\hbar^2)(E - V_i)}$$
$$l_i = x_{i+1} - x_i$$

and

$$Z_{0i} = \frac{2\gamma_i\hbar}{jm_i}$$

is the characteristic impedance of the medium. The above equations express the QMWI at x_i in terms of the QMWI at x_{i+1}, and γ_i, l_i, and Z_{0i}. Once the $Z(x_i)$ is calculated, we can repeat the process for segment $i-1$ to calculate $Z(x_{i-1})$ using γ_{i-1}, l_{i-1}, and Z_{0i-1}. Repeatedly using these equaitons, we can evaluate the total input impedance of the proposed structure and treat the whole superlattices as an equivalent load impedance Z_S. Thus, the reflection coefficient $\rho(E)$ for the wave amplitude can be calculated as

$$\rho(E) = \frac{Z_S - Z_0}{Z_S + Z_0}$$

where Z_0 is the characteristic QMWI of the uniform semiconductor, and the transmission probability is given by

$$T(E) = 1 - |\rho(E)|^2.$$

We have used the above equation to calculate the transmission probability for an EBPF with the identical structure parameters used in Fig. 2. The result is the same as that calculated by the transfer-matrix method, so we will not show it here.

Fig. 8 shows the QMWI, Z_S, and Z_0 as functions of energy for the structure used in Fig. 2. From the transmission line theory [21], we know that matched condition occurs when the load impedance is equal to the characteristic impedance of the transmission line. Under the matched condition, the reflection coefficient is zero and the transmission coefficient is equal to 1. Fig. 8 clearly demonstrates that when the incident energy lies in the passband, Z_S matches Z_0 completely, while outside the passband, large impedance mismatch exists. The result is in good agreement with that calculated in Fig. 2. This explains why the proposed structure has the property of total transmission for a Gaussian wavepacket.

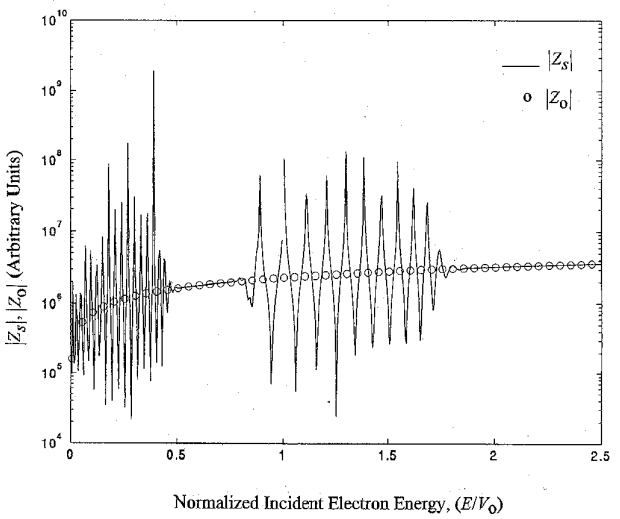

Fig. 8. The absolute values of QMWI Z_S and Z_0 as a function of normalized incident electron energy with the structure parameters used in Fig. 2.

B. Tunneling Time Calculated by QMWI

The tunneling time based on the QMWI can be expressed in an integral form [22]:

$$\tau_{QMWI} = 2\int_0^L \frac{dx}{R(x)}$$

where $R(x)$ is the real part of the QMWI, $Z(x)$, and L is the total tunneling length. The $R(x)$ can be obtained using the method described in Section V-A. Thanikasalam *et al.* [17] have used this method and derived the analytical expressions for tunneling time through single and double barrier structures. The QMWI approach is unique and it can be easily implemented with a numerical method for arbitrary-shaped potential barriers [22]. Since this approach does not involve the nature of the wavepacket, ambiguity results from the wavepacket can be avoided. The EBPF proposed in this paper provides us a chance to examine the accuracy of the tunneling time calculated by this method and compare it with the accurate τ_{WP} presented above. We use the Simpson's rule to evaluate the integral for τ_{QMWI}. Comparison of τ_{WP}, τ_{QMWI}, and τ_{free} (the EBPF is the same as that used in Fig. 2) is shown in Table I. When the incident energy E is $0.65V_o$ (i.e., $E < V_o$), we find that τ_{QMWI} is 0.4485 ps, which is greater than real tunneling time, τ_{WP} (= 0.4072 ps). It is interesting to note [17] that the calculated τ_{QMWI} is always greater than those obtained from other theoretical approaches. Although τ_{QMWI} is not equal to τ_{WP}, they are all greater than the free-particle transit time τ_{free} (= 0.3277 ps). The tunneling time obtained from some approaches may be below τ_{free} for a range of incident energies [17], which lead us to question

TABLE I
COMPARISON OF THE TUNNELING TIME τ_{WP}, τ_{QMWI} FOR THE ENERGY BANDPASS FILTER AND THE FREE PARTICLE TIME τ_{free}

	$E = 0.65\ V_0$	$E = 2.25\ V_0$
τ_{WP}	0.4072 ps	0.1891 ps
τ_{QMWI}	0.4485 ps	0.1982 ps
τ_{free}	0.3277 ps	0.1762 ps

the physical content of these approaches. When the incident energy E is $2.25V_o$, (i.e., $E > V_o$), the calculated τ_{QMWI} is 0.1982 ps, which is greater than τ_{WP} (= 0.1891 ps), but the difference is small. Both τ_{QMWI} and τ_{WP} are also greater than τ_{free} (= 0.1762 ps). It is reasonable since the electron is moving in a classically allowed region. It was shown that τ_{QMWI}, which is based on the concept of group velocity, gives physically meaningful results in the limits of zero and infinite incident electron energy [17]. From our numerical results, we believe the free particle time τ_{free} is always less than the traversal time with the presence of potential barriers for all incident energies.

VI. CONCLUSION

An artificial quantum-mechanical energy bandpass filter using a superlattice structure with a gradually changing barrier and well width has been proposed. Adjustable flat transmission bands and reflection bands are obtained by properly choosing the layer parameters. When an electron impinges upon the proposed structure, it is completely reflected or transmitted depending on whether the incident energy lies in the stopband or passband of the transmission spectrum. Application of the WKB approximation gives a reasonable explanation of the abrupt change of the transmission profile. We have performed the numerical simulations of wavepacket propagating through an energy bandpass filter to obtain the electron tunneling time under the condition of total transmission, and the ambiguity results from the nature of the wavepacket can be totally avoided in this way. The phenomenon of total transmission can be successfully explained by using the concept of wave impedance analogous to that in the transmission line theory. A comparison of the tunneling time τ_{WP} with the free wavepacket traveling time τ_{free} and the tunneling time τ_{QMWI} based on the QMWI method has been presented. τ_{WP} is found to be always greater than τ_{free}. The extra time is due to the electron bouncing back and forth within the barrier system.

REFERENCES

[1] H.-H. Tung and C.-P. Lee, "An energy band-pass filter using superlattice structures," *IEEE J. Quantum Electron.*, vol. 32, pp. 507–512, 1996.

[2] H. Kogelnik, "Filter response of nonuniform almost-periodic structures," *Bell Syst. Tech. J.*, vol. 55, pp. 109–126, 1976.

[3] K. Iga, H. Uehara, and F. Koyama, "Electron reflectance of muitiple quantum barrier (MQB)," *Electron. Lett.*, vol. 22, pp. 1008–1010, 1986.

[4] S. T. Yen, C. M. Tsai, C. P. Lee, and D. C. Liu, "Enhancement of electron-wave reflection by superlattices with multiple stacks of multiquantum barriers," *Appl. Phys. Lett.*, vol. 64, pp. 1108–1110, 1994.

[5] F. Capasso, K. Mohammed, and A. Y. Cho, "Resonant tunneling through double barriers, perpendicular quantum transport phenomena in superlattices, and their device applications," *IEEE J. Quantum Electron.*, vol. QE-22, pp. 1853–1869, 1986.

[6] D. Mukherji and B. R. Nag, "Band structure of semiconductor superlattices," *Phys. Rev. B*, vol. 12, pp. 4338–4345, 1975.

[7] M. Lundstrom, *Fundamental of Carrier Transport*. Reading, MA: Addison-Wesley, 1990, pp. 10–11.

[8] T. Nakagawa, N. J. Kawai, and K. Ohta, "Design principles for chirp superlattice devices," *Superlattices and Microstructures*, vol. 1, pp. 187–192, 1985.

[9] E. Merzbacher, *Quantum Mechanics*. New York: Wiley, 1970, pp. 125–126.

[10] A. Goldberg. H. M. Schey, and J. L. Schwartz, "Computer-generated motion pictures of one-dimensional quantum-mechanical transmission and reflection phenomena," *Amer. J. Phys.*, vol. 35, pp. 177–186, 1967.

[11] D. Bohm, *Quantum Theory*. New York: Prentice-Hall, 1952, pp. 260–261.

[12] E. P. Wigner, "Lower limit for the energy derivative of the scattering phase shift," *Phys. Rev.*, vol. 98, pp. 145–147, 1955.

[13] F. T. Smith, "Lifetime matrix in collision theory," *Phys. Rev.*, vol. 118, pp. 349–356, 1960.

[14] M. Buttiker and R. Landauer, "Traversal time for tunneling," *Phys. Rev. Lett.*, vol. 49, pp. 1739–1742, 1982.

[15] M. Buttiker, "Lamor precession and the traversal time for tunneling," *Phys. Rev. B*, vol. 27, pp. 6178–6188, 1983.

[16] D. Sokolovski, S. Brouard, and J. N. L. Connor, "Traversal-time wavefunction analysis of resonance and nonresonace tunneling," *Phys. Rev. A*, vol. 50, pp. 1240–1256, 1994.

[17] P. Thanikasalam, R. Venkatasubramanian, and M. Cahay, "Analytical expression for tunneling time through single and double barrier structures," *IEEE J. Quantum Electron.*, vol. 29, pp. 2451–2458 1993.

[18] E. H. Hauge, J. P. Falck, and T. A. Fjeldly, "Transmission and reflection times for scattering of wave packets off tunneling barriers," *Phys. Rev. B*, vol. 36, pp. 4203–4214, 1987.

[19] N. Teranishi, A. M. Kriman, and D. K. Ferry, "Tunneling by electron packet with an initially sharp wavefront," *Superlatticed and Microstructures*, vol. 3, pp. 509–514, 1987.

[20] A. N. Khondker, M. R. Khan, and A. F. M. Anwar, "Transmission line analogy of resonance tunneling phenomena: The generalized impedance concept," *J. Appl. Phys.*, vol. 63, pp. 5191–5193 1988.

[21] D. K. Cheng, *Field and Wave Electromagnetics*. Reading, MA: Addison-Wesley, 1983, pp. 390–395.

[22] A. F. M. Anwar, A. N. Khondker, and M. R. Khan, "Calculation of the traversal time in resonant tunneling devices," *J. Appl. Phys.*, vol. 65, pp. 2761–2765, 1989.

Hsin-Han Tung, for photograph and biography, see p. 512 of the March issue of this JOURNAL.

Chien-Ping Lee (M'80–SM'94), for photograph and biography, see p. 512 of the March issue of JOURNAL.